SURFACE FLOW ANALYSIS OF TYPHOON 10 INDUCED SLOPE FAILURE BASED ON DIGITAL ELEVATION MODELING

Yulong ZHU [1], Tatsuya ISHIKAWA [2] and Yasuyuki SHIMIZU [3]

[1] Graduate School of Engineering, Hokkaido University (Kita 13, Nishi 8, Kita-ku, Sapporo 060-8628, Japan)
E-mail: zhuyulong@eis.hokudai.ac.jp
[2] Faculty of Public Policy, Hokkaido University (Kita 13, Nishi 8, Kita-ku, Sapporo 060-8628, Japan)
[3] Faculty of Engineering, Hokkaido University (Kita 13, Nishi 8, Kita-ku, Sapporo 060-8628, Japan)

***Key Words**: wide-area surface flow, Nays2D Solver, slope failure, Typhoon, digital elevation modeling*

1. INTRODUCTION

With the intensification of global warming, the extreme weather induced disasters become more and more frequent. Especially, the collapse of slopes caused by typhoon-induced torrential rain continues to increase in Japan. It is worth noting that during August 29th-31st, 2016, Typhoon 10 hit Hokkaido closely following three other typhoons. According to the Japanese Meteorological Agency (JMA), during this period, the observed rainfall in three days peaked at 55 mm and the cumulative rainfall reached 488 mm, which caused the occurrence of several serious roadside slope failures, embankment collapses and debris flows near Nissho pass along the National Highway 274 in Hokkaido. Note that the generation of runoff played an important role in the slope instability.

The mechanism and calculation methods for the generation of surface flow have attracted attention over the last decades[1),2),3),4)]. In this study, wide-area surface flow analysis is used to simulate runoff in the mountain regions from the received rainfall data during Typhoon 10 by employing both hydrologic analysis using GIS software and two-dimensional (2D) plane flow simulation using Nays2D Flood solver of the iRIC software. The numerical simulation approach used in this study by integrating wide-scale runoff analysis with digital elevation modelling is found to reproduce the real phenomenon of runoff generation with rational precision, which is of great significance for evaluating the effect of runoff on slope failure.

2. GOVERNING PROCESSES & EQUATIONS

(1) Kinematic-wave overland flow equations

It typically uses the kinematic wave equation to describe Hortonian surface flow. By combining the Manning equation, it can excellently approximate most overland flow conditions[6),7)]. As shown in **Fig. 1**, the mass balance equation of 1-dimentional is.

$$\frac{\partial h}{\partial t} + \frac{\partial (Uh)}{\partial l} = r \tag{1}$$

$$U = ah^{m-1} \text{ and } a = B\frac{S^{1/2}}{n_{man}} \tag{2}$$

where, h is water depth (m), t is time (s), n_{man} is Manning's coefficient, U is velocity of water (m/s), S is slope, equals to the surface elevation gradient, l stands for the distance coordinate over the slope surface (m), the value of parameter m is taken as 5/3 for turbulent flow, B is a conversion constant which has the value of 1 and units of ($m^{1/3}/s$), r denotes rainfall intensity (m/s).

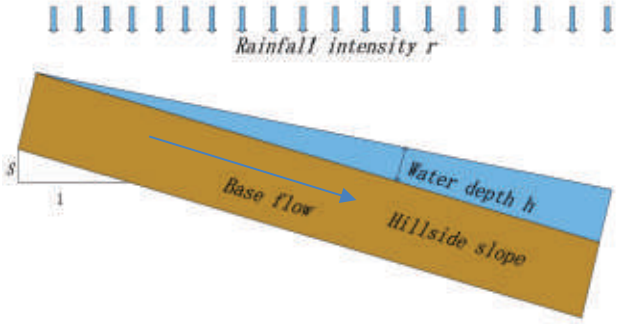

Fig.1 Conceptual schematic of the runoff flow model.

Table 1 SRM and Nays2D Flood Parameters.

Parameter	Value
c_1	12.501
c_2	0.134
c_3	1.752
λ	0.019
p_1	0.600
p_2	0.465

(2) Governing equations of plane flow

The basic equation of a synthetic storage routing model is given by the following Equation[8].

$$\begin{cases} \frac{ds_{to}}{dt} = r - q - b - q_b \\ s_{to} = k_{11} q^{p_1} + k_{12} \frac{d}{dt}(q^{p_2}) \\ b = k_{13} q \\ q_b = q_i \, exp(-\lambda t) \end{cases} \quad (3)$$

in which,

$$\begin{cases} k_{11} = c_1 A^{0.24} \\ k_{12} = c_2 k_{11}^2 (r_1)^{-0.2648} \\ k_{13} = c_3 - 1 \end{cases} \quad (4)$$

where, s_{to} is storage (mm); q is observed runoff (mm/h); b is loss, which is infiltration rate from upstream to downstream (mm/h); q_b is base flow (mm/h); q_i is initial runoff (mm/h); k_{11} and k_{12} are storage parameters, k_{13} is loss parameter, p_1 and p_2 are storage indices; λ is damping factor; A is area of the catchment (km^2); r_1 is mean rainfall intensity (mm/h); c_1, c_2 are c_3 are model parameters.

Some of these parameters were selected since they are average for the entire Hokkaido as shown in **Table 1**.

The following are the basic equations in a rectangular coordinate system (x, y) used in the Nays2D Flood solver[5]:

Equation of continuity:

$$\frac{\partial h}{\partial t} + \frac{\partial (hu)}{\partial x} + \frac{\partial (hv)}{\partial y} = I + r \quad (5)$$

Equations of motion:

$$\frac{\partial (uh)}{\partial t} + \frac{\partial (hu^2)}{\partial x} + \frac{\partial (huv)}{\partial y} = -hg\frac{\partial H}{\partial x} - \frac{\tau_x}{\rho} + D^x \quad (6)$$

$$\frac{\partial (vh)}{\partial t} + \frac{\partial (huv)}{\partial x} + \frac{\partial (hu^2)}{\partial y} = -hg\frac{\partial H}{\partial y} - \frac{\tau_y}{\rho} + D^y \quad (7)$$

$$\text{where: } \frac{\tau_x}{\rho} = C_f u\sqrt{u^2+v^2}; \frac{\tau_y}{\rho} = C_f v\sqrt{u^2+v^2} \quad (8)$$

$$D^x = \frac{\partial}{\partial x}\left[v_t \frac{\partial (uh)}{\partial x}\right] + \frac{\partial}{\partial y}\left[v_t \frac{\partial (uh)}{\partial y}\right] \quad (9)$$

$$D^y = \frac{\partial}{\partial x}\left[v_t \frac{\partial (vh)}{\partial x}\right] + \frac{\partial}{\partial y}\left[v_t \frac{\partial (vh)}{\partial y}\right] \quad (10)$$

where, h is water depth (m), u is water velocity in the x-direction (m/s), v is water velocity in the y-direction (m/s), g is gravitational acceleration, H is water surface elevation (m), τ_x is riverbed shear stress in the x-direction (kPa), τ_y is riverbed shear stress in the y-direction (kPa), C_f is riverbed friction coefficient which has the value of 0.150 for Hokkaido, v_t is eddy viscosity coefficient, ρ is density of water (kg/m^3), I is inflow through a box culvert, a sluice pipe or a pump per unit area (m/s).

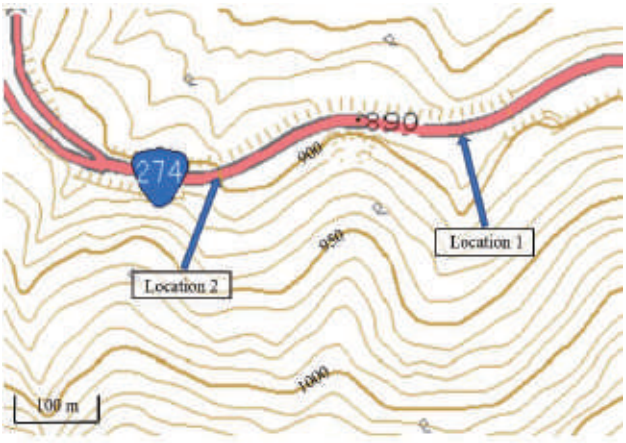

(a) 10m data.

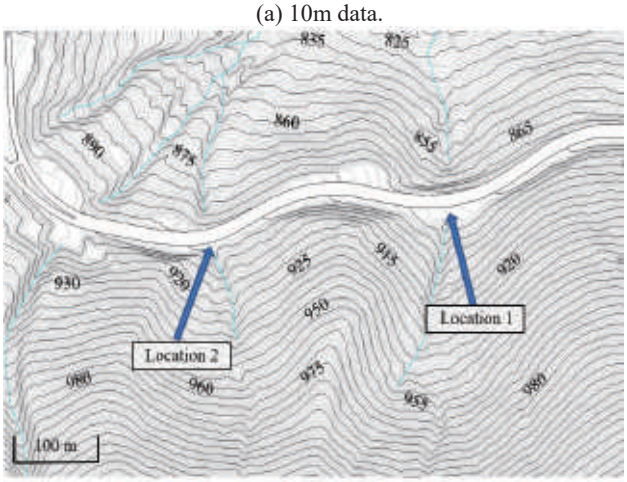

(b) 1m data.

Fig.2 Topographic map of Nissho pass.

3. SURFACE FLOW ANALYSIS

Rainfall will exceed the infiltration capacity of the ground surface and drain in the form of runoff during rainstorm or torrential rain. The high value of runoff velocity will erode exposed surfaces, which may facilitate the initiation and enlargement of debris flow. In the simulation of this process, wide-area surface flow analysis using iRIC is capable in the estimation of the generation of runoff based on digital elevation modeling.

(1) Digital elevation modeling

The slope failure occurred at Location 1 and Location 2 during Typhoon 10 which is labeled in **Fig. 2**, referring to the disaster report[9].

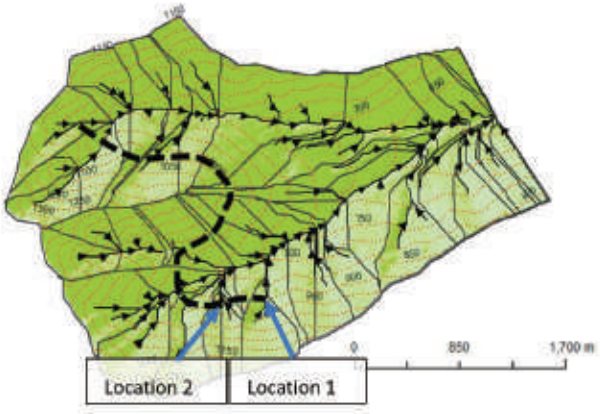

Fig.3 Drainage network and watershed of the site.

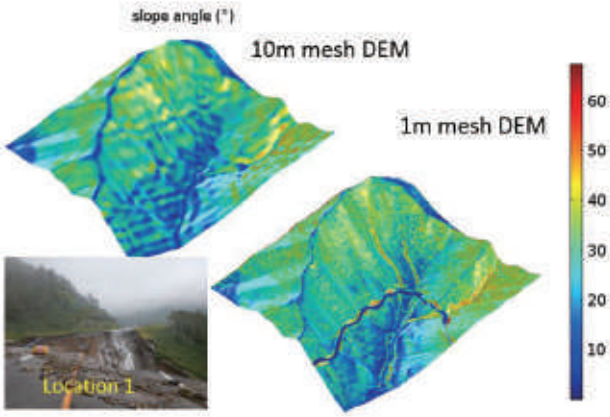

Fig.4 Distribution of slope angle.

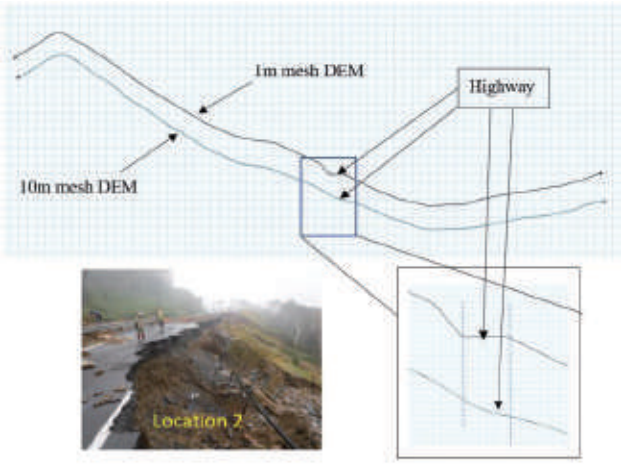

Fig.5 Cross section of Location 2.

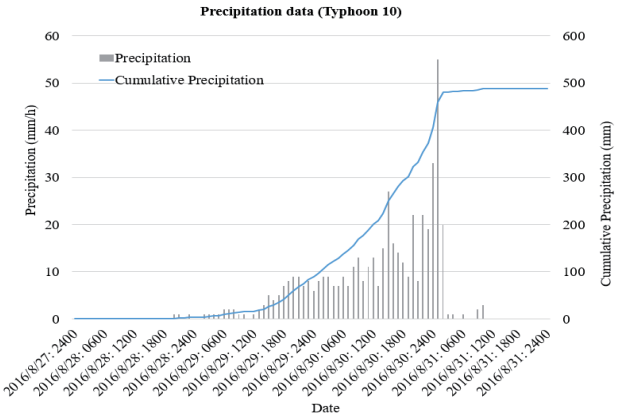

Fig.6 Observed rainfall at the site during Typhoon 10.

Runoff flowing from Location 2 to Location 1 on the highway may be the main reason for the enlargement of the embankment collapse with the length of 100m. Due to the fact that the previous study in this area[10] has not consider the flow of runoff along the highway, it is necessary to actually reproduce runoff. For this purpose, the digital elevation model (DEM) using 10m data (**Fig. 2(a)**), which was sourced from Geospatial Information Authority of Japan, is compared with the DEM using 1m laser profile data (**Fig. 2(b)**) from Hokkaido Regional Development Bureau to discuss the influence of terrain accuracy on runoff. National Highway 274 (black dashed line) shown in **Fig. 3** is situated along the hillside slope, where will be eroded by the runoff that flows from the top of the mountain, especially in the valley's catchment area like Location 1 and Location 2. The drainage network is outlined by using GIS software, shown in arrowed lines and the solid lines are stream lines in this watershed. **Fig. 4** shows the distribution of slope angle of both 10m and 1m mesh DEM. It can be observed that the hillside slope next to Highway 274 is very steep with an average slope of 30 degrees, suggesting that the runoff water will erode the exposed surface with high velocity, and results in the generation of debris flow at Location 1. As a large amount of runoff water is generated on the Highway surface, the road shoulder is eroded and the surface water seeps into the embankment, which increases pore water pressure and decreases shear strength of embankment. Therefore, the water flow from the Location 2 direction along the Highway 274 may cause the initiation and enlargement of embankment collapse[9]. It is also recognizable that from **Fig. 5** that the shape of the highway is more clearer with 1m mesh DEM, which implies that the runoff flowing along the highway will be more accurately calculated.

(2) Climatic condition

From 01:00 on August 29th to 23:00 on the August 31st, 2016, Typhoon 10 hit Hokkaido following three other typhoons (No.7, No.11, No.9). The observed precipitation data measured by the Kaihatsukyoku's telemeter near the site are shown in **Fig. 6**. It is recognizable that the observed rainfall peaked at 55 mm on 24:00 at 30th of August 2016 and the maximum observed cumulative rainfall as shown by the light blue line exceeded 500 mm which far exceeds the average August rainfall in the area.

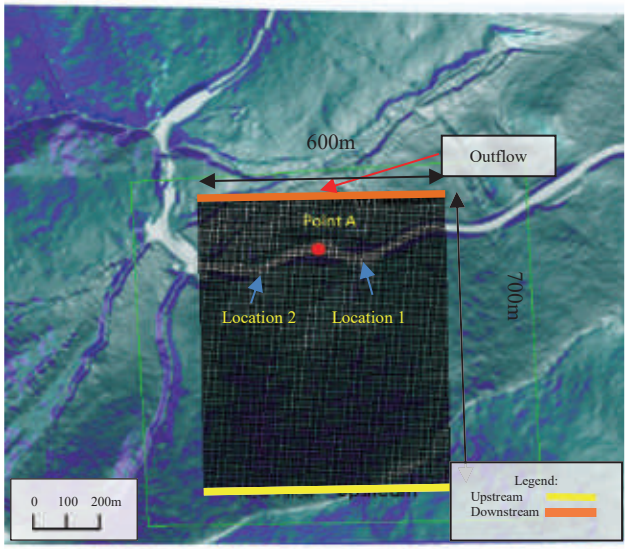

Fig.7 iRIC – Nays2d Flood analysis model.

(3) Surface flow analysis by using iRIC

The surface flow analyses we conducted using Nays2D Flood solver of the iRIC software. Nays2D is a plane 2D solver for calculating flow, sediment transport, bed evolution and bank erosion in rivers[5]. In this study, there are two different digital elevation models, namely 10m and 1m mesh DEM, are used in surface flow simulations for comparative analysis of runoff generation along the Highway 274. The model that calculated in iRIC is shown in **Fig. 7**. The black grid part is the calculation domain and it is applied rainfall data as boundary conditions. The red point A is located on the center of Highway 274 and it will be used as a representative point to analyze the depth of the water flowing from Location 2 to Location 1. As the watershed has a significant effect on the runoff in the drainage area, the calculation area is set within the range of 600m×700m to ensure that the runoff water of the drainage network in the scope of the calculation domain could be able to come from all upstream watershed of Location 1 and Location 2.

4. RESULS & DISCUSSIONS

Fig. 8 and **Fig. 9** show the distribution of water depth. Since both Location 1 and Location 2 are located at the exit of the valley, where the water from the watershed on both sides is gathered, the water depth is much higher than other parts of the highway so that embankment erosion is enhanced leading to the occurrence of slope failure. Especially, in **Fig.8**, it can be identified that the water depth in a large upstream area of Location 1 exceeds 200mm, which could cause severe erosion of the exposed hillside, particularly in the case of steep slope with the inclination angle of 30 degrees.

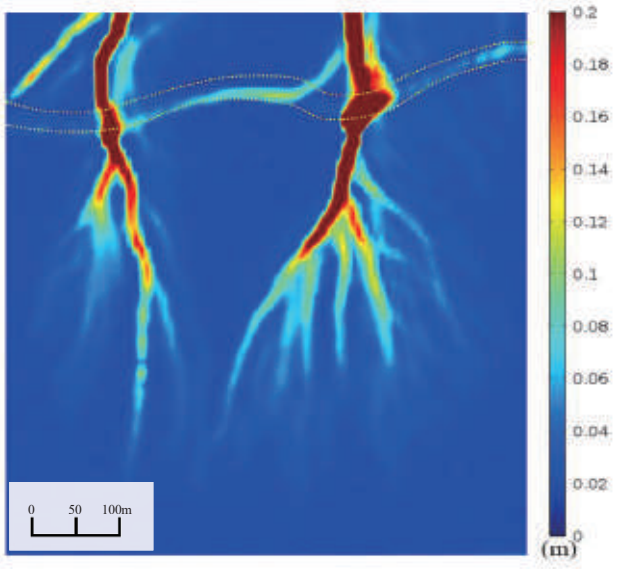

Fig.8 Distribution of water depth(1m mesh DEM).

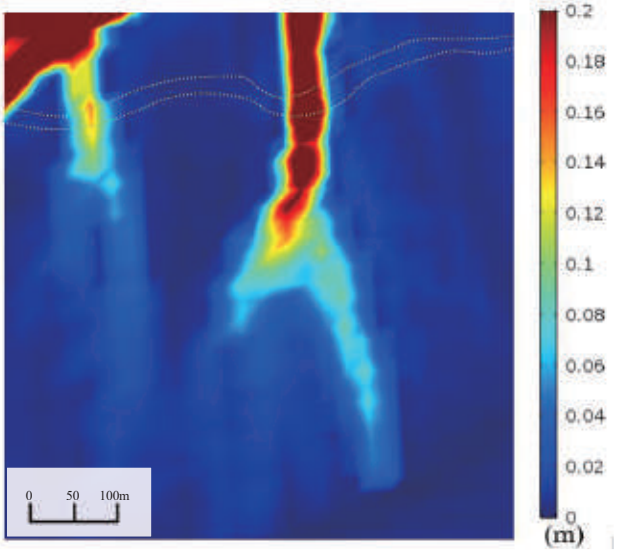

Fig.9 Distribution of water depth(10m mesh DEM).

From **Fig. 8** it also can be identified that there is significant water accumulation on the highway (shown by dotted line), meaning that runoff flows along the highway. However, in the same area of the highway, the water depth is not clearly displayed in **Fig. 9**. The maximum water depth calculated by iRIC are 1.275m and 0.181m at Location 1 with the sevenfold difference as shown in **Fig. 10**. On the other hand, at Location 2, the maximum water depth are 0.479m and 0.117m respectively with the four times difference. The changes in water depth and rainfall are consistent both at Location 1 and Location 2. At Location 1 with 1m mesh DEM, it is recognizable that the water depth has a steep increase followed by a slight change at 18:00 on August 28th. When the calculated terrain in iRIC is selected to use 10m mesh DEM, it can be seen that there is no significant difference in water depth at Location 1 and Location 2, which implies the runoff could not flow from Location 2 to Location 1 along the highway.

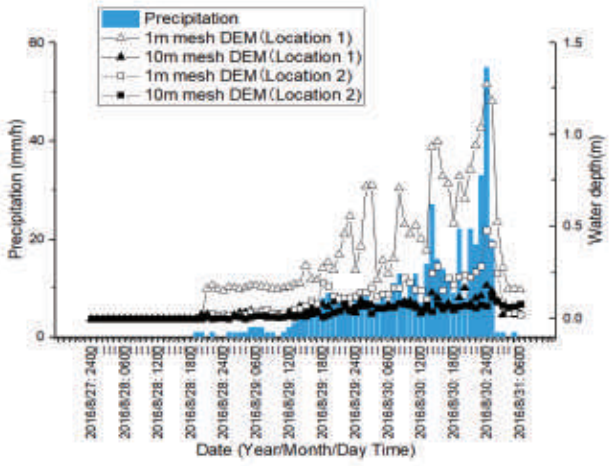

Fig.10 iRIC calculations of water depth at each Location.

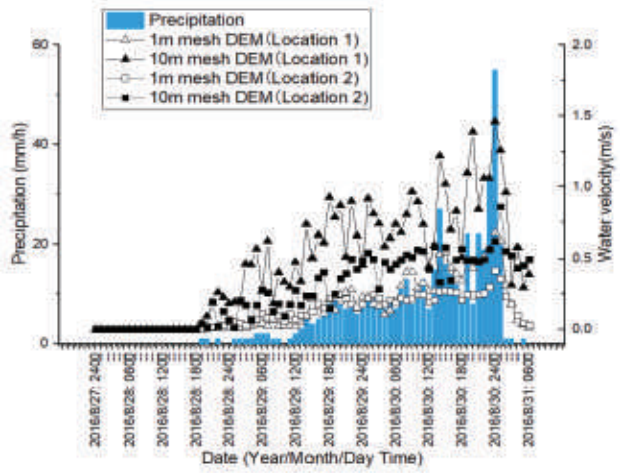

Fig.12 iRIC calculations of water velocity at each Location.

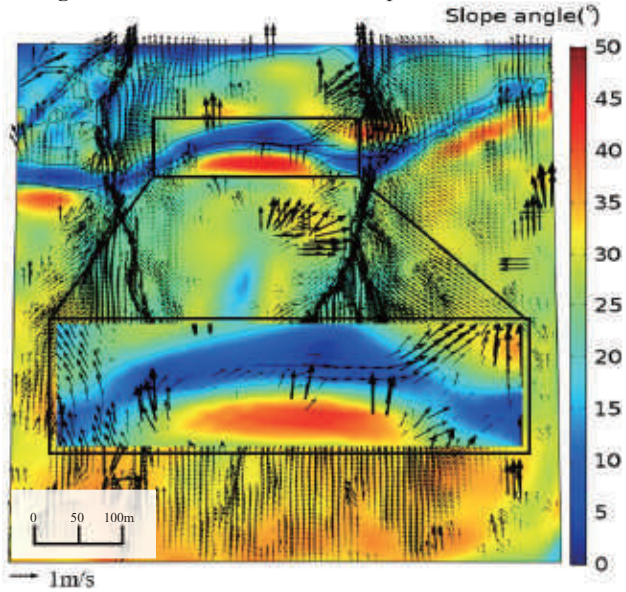

Fig.11 Distribution of water velocity(1m mesh DEM).

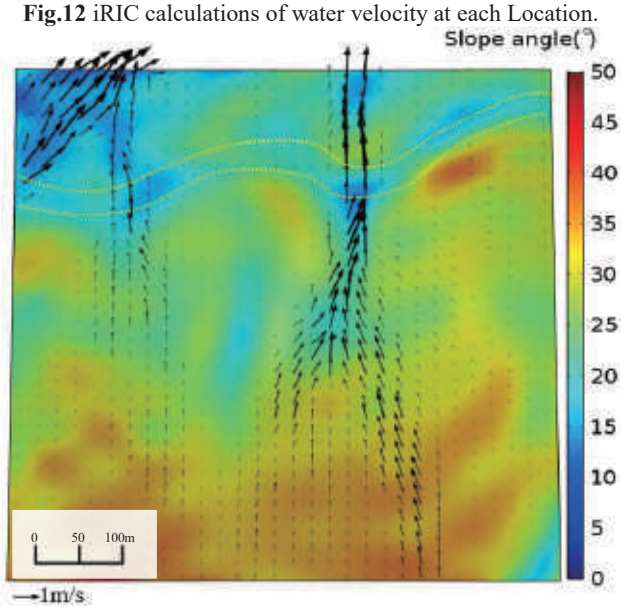

Fig.13 Distribution of water velocity(10m mesh DEM).

However, the maximum value of water head difference between Location 1 and Location 2 is 0.796m at 24:00 on August 30th as shown in **Fig.10.** When it is selected to use 1m mesh DEM, meaning that water on the Highway 274 will be driven by the water head, and runoff will be generated. The direction of the water velocities with 1m and 10m mesh DEM are displayed as black arrow in **Fig. 11** and **Fig. 13** respectively. The length of the arrow indicates the magnitude of velocity. The legends show the slope angle of the hillside. In **Fig. 11**, the generation of runoff on the Highway is identifiable. It can be observed in **Fig.11** that due to the larger slope angle of the hillside, the water velocity on the hillside between Point A and Location 1 is large, but water depth is very small in the same area as shown in **Fig. 8**. It caused the average discharge, which could be treated as water depth times water velocity, is relatively small on the hillside ($3.3\times10^{-4}m^3/s$) compared to the average discharge on the highway ($4\times10^{-3}m^3/s$). Therefore, the runoff water on the highway is mainly flows from Location 2 to Location 1, and merges with the water flowing out of the valley and flows downstream together, which is consistent with the actual picture shown in **Fig. 4**. **Fig. 12** shows the water velocity at Location 1 and Location 2 with two different terrain conditions, 1m and 10m mesh DEM respectively. The maximum value of water velocity is 0.677m/s (1m mesh DEM) and 1.460m/s (10m mesh DEM) at Location 1, and for Location 2, the maximum value of water velocity is 0.416m/s (1m mesh DEM) and 0.860m/s (10m mesh DEM) respectively. The maximum magnitude of water velocity at Location 1 and Location 2 with 10m mesh DEM are almost twice as fast as 1m mesh DEM, and this can be attributed to the effect of slope. When the water velocity is small, water cannot be quickly drained, resulting in the increase of water depth, which reduces the slope stability[10]. From **Fig. 13**, it can only be roughly seen that runoff water flows from the watershed to the valley first, and then flows from the upstream to the downstream. In addition, a representative point (Point A) located in the center of the Highway 274 between Location 1

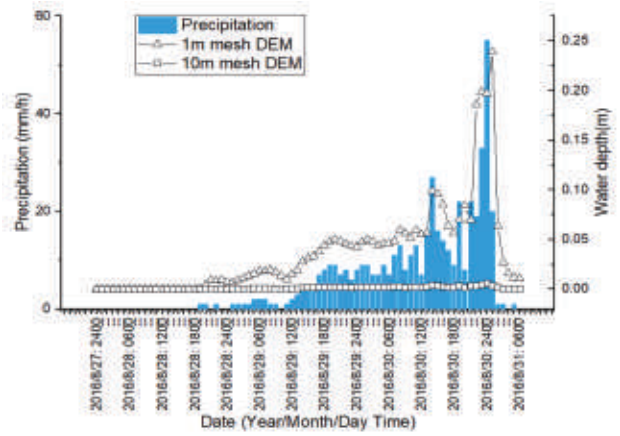

Fig.14 iRIC calculations of water depth at Point A.

and Location 2 is selected for analysis the runoff on the Highway 274. **Fig. 14** shows the change of the water depth for runoff at Point A during Typhoon 10. It is recognizable that the water depth at Point A is 0.239m and 0.012m respectively with 1m and 10m mesh DEM, meaning that the 1m mesh DEM reproduced the generation of runoff flows from Location 2 to Location 1 along the Highway 274. The most important difference between 1m mesh DEM and 10m mesh DEM is the shape of the highway, but the terrain difference for hillside areas between 1m mesh DEM and 10m mesh DEM is not significant, as shown in **Fig.5**. Therefore, theoretically an intermediate method that only refining the terrain features of the highway in 10m mesh DEM is feasible. However, the biggest difficulty is that the boundary of the highway cut from the 1m mesh DEM cannot be bonded with the boundary of the 10m mesh DEM after cut off the highway, and it still needs further investigation. In addition, the infiltration is a two-stage process during a rainfall event. When the rainfall intensity is lower than the infiltration capacity at the beginning of the rainfall, all the rainfall infiltrates into the soil. As rainfall continues, when the rainfall intensity equals to or greater than infiltration capacity, runoff will be generated on the surface of the soil. In this study, the two-stage process of infiltration is not considered, and infiltration is considered as a constant rate. Therefore, considering this two-stage process of infiltration in the runoff analysis is the future work in the related research.

5. CONCLUSION

In order to estimate the runoff impact of the slope failure caused by Typhoon 10 in Hokkaido, 2016, wide-area runoff analysis was used with two different DEMs, 1m and 10m mesh DEM respectively, to simulate the runoff caused by rainfall in mountain areas. The results show that higher-precision terrain information will be able to more realistically simulate the flow of runoff. After the occurrence of runoff, there was a large amount of water flow along the valleys of mountainous regions and Highway 274 from Location 2 to Location 1. The numerical modelling approach used in this study by integrating wide-scale runoff analysis with digital elevation modelling is found to reproduce the real phenomenon of runoff generation with rational precision.

ACKNOWLEDGMENT: We acknowledge Hokkaido Regional Development Bureau for providing the bulk information used in this research gratefully. This research was supported in part by Grant-in-Aids for Scientific Research (A) (16H02360) from Japan Society for the Promotion of Science (JSPS) KAKENHI.

REFERENCES

1) Abdul, A.S. and Gillham, R.W.: Laboratory studies of the effects of the capillary fringe on streamflow generation. Water Resour. Res., Vol. 20, pp. 691-698, 1984.

2) Beven, J.B.: Rainfall–Runoff Modelling. Wiley, New York, 2001.

3) Li, Z. and Zhang, J.: Calculation of field manning's roughness coefficient. Agric. Water Manage. Vol.49, pp.153-161, 2001.

4) Weill, S., Mouche, E. and Patin, J.: A generalized Richards equation for surface/subsurface flow modelling, Journal of Hydrology, Vol.366, pp.9-20, 2009.

5) Shimizu, Y., Inoue, T., Suzuki, E., Kawamura, S., Iwasaki, T., Hamaki, M., Omura, K., Kakegawa, E. and Yoshida, T.: Nays2D Flood Solver Manual, 2014.

6) Martin, J.L. and McCutcheon, S.C.: Hydrodynamics and Transport for Water Quality Modeling. CRC Press, Inc., Boca Raton, FL pp. 7-220, 1999.

7) Gottardi, G. and Venutelli, M.: A control-volume finite element model for two-dimensional overland flow. Adv. Water Resour. Vol.16, pp.227-84, 1993.

8) Runoff Calculation SRM Solver Manual, International River Interface Cooperative (iRIC), 2014.

9) Japanese Geotechnical Society. The final report of ground disaster investigation report due to heavy rain in Hokkaido during August 2016. (in Japanese) , 2017.

10) Zhu Y.L., Siva Subramanian S. and Ishikawa T.: Evaluating Applicability of Coupled Numerical Methods for Slope Runout Analysis, 58th Annual meeting of Hokkaido Branch Japanese Geotechnical Society. pp.309-318, 2018.

(Received May 18, 2018)